A Nitroxide Radical Conjugated Polymer as an Additive to Reduce Nonradiative Energy Loss in Organic Solar Cells

ADVANCED MATERIALS
www.advmat.de

A Nitroxide Radical Conjugated Polymer as an Additive to Reduce Nonradiative Energy Loss in Organic Solar Cells

Furong Shi, Pengzhi Guo, Xianfeng Qiao, Guo Yao, Tao Zhang, Qi Lu, Qian Wang, Xiaofeng Wang, Jasurbek Rikhsibaev, Ergang Wang, Chunfeng Zhang,* Young-Wan Kwon, Han Young Woo,* Hongbin Wu, Jianhui Hou, Dongge Ma, Ardalan Armin, Yuguang Ma, and Yangjun Xia**

Nonfullerene-acceptor-based organic solar cells (NFA-OSCs) are now set off to the 20% power conversion efficiency milestone. To achieve this, minimizing all loss channels, including nonradiative photovoltage losses, seems a necessity. Nonradiative recombination, to a great extent, is known to be an inherent material property due to vibrationally induced decay of charge-transfer (CT) states or their back electron transfer to the triplet excitons. Herein, it is shown that the use of a new conjugated nitroxide radical polymer with 2,2,6,6-tetramethyl piperidine-1-oxyl side groups (GDTA) as an additive results in an improvement of the photovoltaic performance of NFA-OSCs based on different active layer materials. Upon the addition of GDTA, the open-circuit voltage (V_{OC}), fill factor (FF), and short-circuit current density (J_{SC}) improve simultaneously. This approach is applied to several material systems including state-of-the-art donor/acceptor pairs showing improvement from 15.8% to 17.6% (in the case of PM6:Y6) and from 17.5% to 18.3% (for PM6:BTP-eC9). Then, the possible reasons behind the observed improvements are discussed. The results point toward the suppression of the CT state to triplet excitons loss channel. This work presents a facile, promising, and generic approach to further improve the performance of NFA-OSCs.

1. Introduction

Over the last decades, bulk heterojunction organic solar cells (OSCs) comprised of blends of electron donors (D) and acceptors (A) have attracted great attention because of their potential for realizing low-embodied energy, solution-processed, and flexible solar cells tailorable for a variety of application targets.[1–4] Variety of approaches such as the development of numerous D- and A-materials,[5–12] and optimization of the device fabrication processes and device configurations have been extensively implemented to achieve high-performance OSCs.[1,13–16] However, the power conversion efficiencies (PCEs) of OSCs are still considerably lower than their inorganic and organic–inorganic hybrid counterparts.[17–19] The lower PCEs of fullerene-based OSCs are found to be mainly due to the voltage loss as a result of the typically large interfacial energy offset required for photoinduced exciton

F. Shi, P. Guo, Q. Lu, Q. Wang, X. Wang, J. Rikhsibaev, Y. Ma, Y. Xia
Organic Semiconductor Materials and Applied Technology Research Centre of Gansu Province
School of Materials Science and Engineering
Lanzhou Jiaotong University
Lanzhou 730070, P. R. China
E-mail: xiayangjun2015@126.com

P. Guo
National Green Coating Equipment and Technology Research Centre
Lanzhou Jiaotong University
Lanzhou 730070, P. R. China

The ORCID identification number(s) for the author(s) of this article can be found under https://doi.org/10.1002/adma.202212084

DOI: 10.1002/adma.202212084

X. Qiao, H. Wu, D. Ma
State Key Laboratory of Luminescent Materials and Devices
South China University of Technology
Guangzhou 510640, P. R. China

G. Yao, C. Zhang
National Laboratory of Solid-State Microstructures
School of Physics
and Collaborative Innovation Center for Advanced Microstructures
Nanjing University
Nanjing 210093, P. R. China
E-mail: cfzhang@nju.edu.cn

T. Zhang, J. Hou
State Key Laboratory of Polymer Physics and Chemistry
Beijing National Laboratory for Molecular Sciences CAS
Research/Education Center for Excellence in Molecular Sciences
Institute of Chemistry Chinese Academy of Sciences
Beijing 100190, P. R. China

E. Wang
Department of Chemistry and Chemical Engineering
Chalmers University of Technology
Göteborg SE-412 96, Sweden
E-mail: ergang@chalmers.se

dissociation,[20,21] relatively large energetic disorder, and additional energy losses via both radiative and nonradiative recombination of free charges via charge-transfer (CT) states.[21–29] On the contrary, for nonfullerene acceptor-based OSCs (NFA-OSCs), the energy offset between the D and A materials and the energetic disorder can be substantially decreased while charge generation is maintained efficiently. This manifested as higher photovoltages for the given photocurrent values in these systems.[30–32] Such technical advantages have resulted in considerable improvements in the performance of the single junction NFA-OSCs with the highest certified PCE of 17.3%–18.6% 20% in sight and an optimistic value of 25% predicted.[3,33–35] To further improve the efficiency beyond the current values, all loss mechanisms, however small, must be identified and eliminated. The most challenging of these losses to tackle is arguably nonradiative recombination, which seems to be an intrinsic characteristic of organic semiconductors.[3,30-32]

Several mechanisms and/or models have been proposed to describe the nonradiative voltage losses ($V_{oc}^{non-rad}$), to explain their dependence on materials, and device properties and to put forward possible means for overcoming them.[36–45] Accordingly, promising strategies to reduce nonradiative losses have been developed or resurrected from the traditional approaches such as morphology optimization of the photoactive layer, molecular engineering of D- and A-type materials, and forging multiple-component OSCs.[35,46–50] For example, Janssen et al. demonstrated that the improvement of film morphology through solvent additives would mitigate the charge carrier recombination through (dark) triplet states channel hence reducing nonradiative losses.[46] Li, Zhang and Yang et al. separately verified that the nonradiative loss could be suppressed via fluorination of either D or A materials.[47–50] Hou et al. have reported the suppression of nonradiative energy loss ($E_{loss}^{non-rad}$) of OSCs with PCEs approaching 19% by employing a third component.[35]

Different to the said approaches, spin manipulation has been also employed as a strategy. Vardeny et al. employed Galvinoxyl (Gxl) (2,6-di-butyl-*α*-(3,5-di-*tert*-butyl-4-oxo-2,5-cyclohexadiene-1-ylidene)-*p*-tolyloxy) as a spin-manipulating additive in P3HT:PC_{61}BM based OSCs, and they suggested that the Gxl additive facilitate the conversion of singlet CT (^{1}CT) to triplet CT (^{3}CT) states with a longer lifetime which results in a more efficient charge separation efficiency and reduced recombination. This ultimately resulted in improvements in the short-circuit current density (J_{SC}) and the fill factor (FF) of the OSCs.[51,52] Kim et al. argued that the increased efficiency of the P3HT:PC_{61}BM-based OSCs was most likely not due to the increased population of triplet polarons (^{3}CT state) upon the introduction of Gxl additives.[53] Vardeny et al. later extended the application of Gxl as an additive in the OSCs to PTB7:PC_{61}BM blends and achieved a 30% improvement in the PCEs. This, however, resulted in a decrease in the PCE of PTB7:PC_{71}BM blends. They further suggested that Gxl facilitates the intersystem conversion between ^{3}CT state excitons and ^{1}CT state excitons and thereby suppresses the back charge transfer (BCT) from the CT states to the ending lower-lying triplets on PTB7. This ultimately results in the improvement of the photocurrent of the OSCs based on PTB7:PC_{61}BM blends.[54]

In this work, we tackle the problem of nonradiative loss in NFA-based OSCs by utilization of solid radical additive. First, we found that the addition of the Gxl additives, particularly in the case of NFA systems, results in decreased PCEs (Table S1, Supporting Information). In this regard, the effectiveness of the employment of radical additives to increase the photovoltaic performance of OSCs remains ambiguous and needs to be further investigated. Moreover, universally effective strategies such as additives to considerably improve the performance of OSCs, especially in NFA-based OSCs, are yet to advance. In this context, a nitroxide radical conjugated polymer (GDTA) comprising a benzo[1,2-*b*;4,5-*b'*]dithiophene (BDT)-based conjugated backbone with dangling 2,2,6,6-tetramethyl piperidine-1-oxyl (TEMPO) side groups, was successfully prepared and characterized. Upon the addition of 2 wt% GDTA (relative to the weight of PM6), the PCEs of PM6:Y6-based OSCs were improved from 15.8% to 17.6%. In parallel, the strategy is applied to the 10 different additional bulk heterojunction photovoltaic material systems, for which similarly remarkable performance improvements are obtained. The OSCs of particular interest are based on the ternary PM6:BTP-eC9:GDTA (0.5 wt%) blend for which a maximum PCE of 18.3% is achieved. Notably, the reduced $E_{loss}^{non-rad}$, decreased T_1 exciton population in Y6 and increased photostability as well, were observed and supported by a range of optical and electrical spectroscopic measurements of the representative OSCs from PM6:Y6 blends with and without GDTA. The results indicate that the GDTA seemed to act as a generic additive to improve the performance of NFAs-OSCs via the suppression of T_1 formation.

2. Results

2.1. Synthesis and Characterization of GDTA

The synthetic routes of the monomers and the resulting radical polymer GDTA are presented in **Scheme 1**. For comparison, a control polymer GDZZ based on the same polymeric backbone with ethyl ester side groups instead of TEMPO in GDTA was also synthesized. 2,6-Bis(trimethylstannyl)-4,8-bis(4,5-dioctylthiophen-2-yl)benzo[1,2-*b*:4,5-*b'*]dithiophene (BDT-Sn) was synthesized by following a previous report, and characterized before use.[55] 2,5-Dibromo-1,4-bis(4-oxy-2,2,6,6-tetramethylpiperidine-1-oxyl)phthalate (BTMP) was prepared with a yield of 65.4% by coupling 2,5-dibromoterephthalic acid and 4-hydroxy-2,2,6,6-tetramethylpiperidine-1-oxyl (4-OH-TEMPO) radical via Steglich esterification (see detailed discussion in Note S1 in the Supporting Information).[56] The electrospray ionization time-of-flight mass spectrometry (ESI-TOF/MS) measurement confirmed the molar mass of BTMP (Figure S1, Supporting Information). **Figure 1**a displays the

Y.-W. Kwon, H. Y. Woo
Department of Chemistry
KU-KIST Graduate School of Converging Science and Technology
Korea University
Seoul 02841, Republic of Korea
E-mail: hywoo@korea.ac.kr
A. Armin
Sustainable Advanced Materials (Sêr SAM)
Department of Physics
Swansea University
Singleton Park, Swansea SA2 8PP, UK

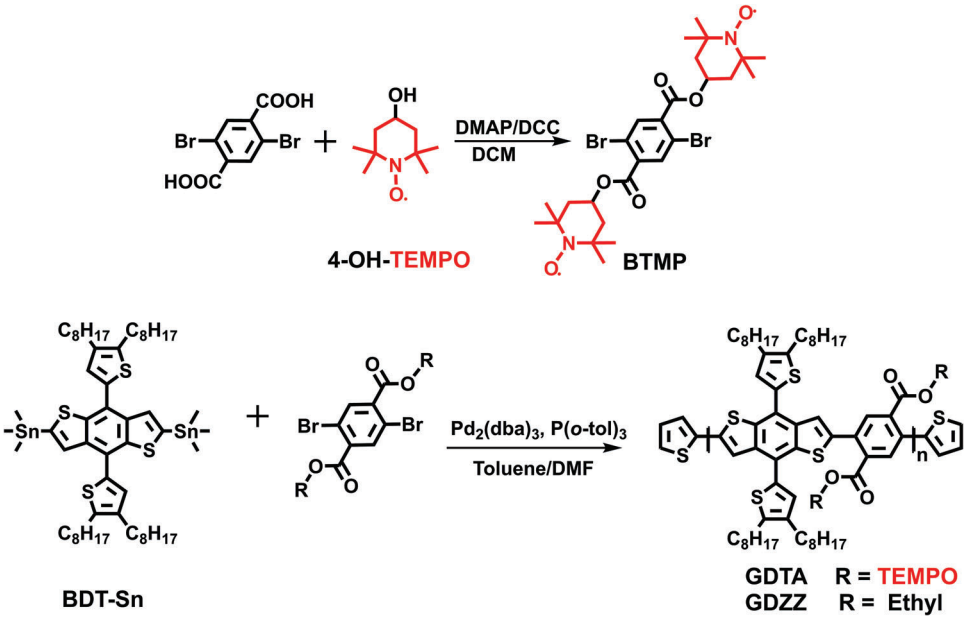

Scheme 1. Synthetic routes of the polymers GDTA and GDZZ.

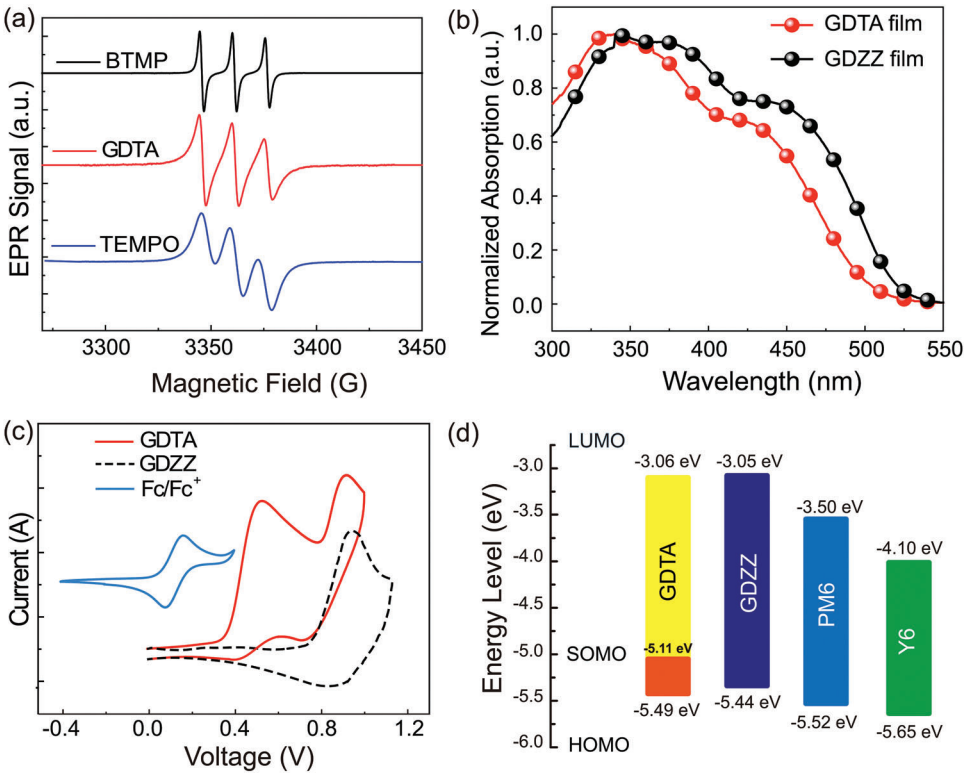

Figure 1. a) EPR spectra of TEMPO, BTMP, and GDTA. b) Normalized absorption spectra of GDTA and GDZZ in film. c) Cyclic voltammograms of GDTA, GDZZ, and Fc/Fc$^+$, and d) energy level diagram of GDTA, GDZZ, PM6, and Y6.

hyperfine structures in the electron paramagnetic resonance (EPR) spectrum of BTMP in tetrahydrofuran (THF) with a $g(Q)$ value of 2.008, where the 3 peaks are interpreted in terms of the hyperfine coupling of the unpaired electron in N–O with ^{14}N nuclear spin in TEMPO radicals.[57,58] To further confirm the molecular structure of BTMP, it was reduced by erythorbic acid to generate 2,5-dibromo-1,4-bis(4-oxy-2,2,6,6-tetramethylpiperidine-1-hydroxyl)phthalate, the structure of which was verified by ^{1}H NMR measurement (Figure S2, Supporting Information). All the ESI-TOF/MS, EPR, and ^{1}H NMR

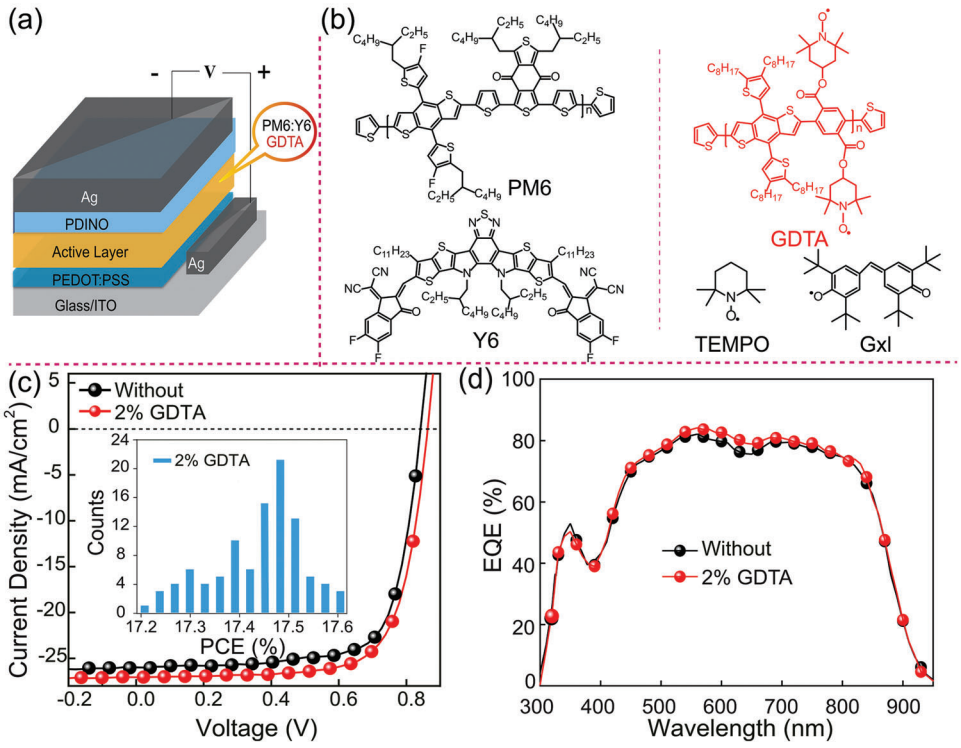

Figure 2. a) Device structure. b) Chemical structures of PM6, Y6, GDTA, TEMPO, and GxI. c) *J–V* curves of PM6:Y6-based OSCs with and without GDTA. d) EQE characteristics of PM6:Y6-based OSCs with and without GDTA.

results confirmed that the monomer BTMP was successfully synthesized.

GDTA and the controlled polymer GDZZ were prepared via palladium-catalyzed Stille coupling between BDT-Sn and BTMP or 2,5-dibromoterephthalic acid diethyl ester with 74% and 77% yields, respectively (see detailed discussion in Note S1 in the Supporting Information).[55] The number-average molecular weight (M_n) and polydispersity index (PDI) were determined to be 14 300 g mol^{-1} and 2.3 for GDTA and 16700 g mol^{-1} and 2.5 for GDZZ (Table S2, Supporting Information), by gel-permeation chromatography (GPC) with THF as eluent relative to polystyrene standards. As shown in Figure 1a, GDTA exhibited an almost identical EPR spectrum to BTMP and TEMPO with a hyperfine structure ($g(Q) = 2.009$) in a dilute THF solution, indicating that the TEMPO moiety was successfully incorporated into the polymer. The successful synthesis of GDTA was also supported by the comparable absorption spectra of GDTA and GDZZ because of the same conjugated backbone (Figure 1b) in the two polymers.

The electrochemical properties of GDTA and GDZZ films were investigated by cyclic voltammetry (CV) as described in the Supporting Information General Method. As shown in Figure 1c, the first and second onset oxidation potentials (E_{OX}) of GDTA were measured to be 0.41 and 0.79 V, respectively. For comparison, the onset of oxidation potentials of the control polymer GDZZ (0.74 V) and TEMPO (0.34 V) was separately determined (Figure 1c; Figure S3, Supporting Information). The results suggested that the E_{OX} of 0.41 and 0.79 V for GDTA might be originated from the oxidation of the dangling TEMPO moieties and the conjugated backbone, respectively. From CV measurements, the singly occupied molecular orbital (SOMO) energy level of dangling radicals in GDTA was determined to be −5.11 eV by the empirical formula of $E_{SOMO} = -(E_{OX}^{Radical} + 4.70)$ (eV), where the redox potential of Fc/Fc$^+$ was + 0.10 eV under the same conditions.[55,57] Similarly, the highest occupied molecular orbital (HOMO) and the lowest unoccupied molecular orbital (LUMO) energy levels of GDTA were calculated to be −5.49 eV and −3.06 eV, respectively, from the oxidation onset (0.79 V) and the corresponding optical bandgap (E_g^{opt}) (2.43 eV) using the empirical formulas $E_{HOMO}^{GDTA} = -(E_{OX}^{GDTA} + 4.70)$ eV and $E_{LUMO}^{GDTA} = -(|E_{HOMO}^{GDTA}| - |E_g^{opt}|)$ eV.[55,59] A similar LUMO energy level (−3.05 eV) and a slightly upshifted HOMO energy level (−5.44 eV) were also calculated for GDZZ as shown in Figure 1d. The results also indicate that a radical conjugated polymer with TEMPO radical species and conjugated backbone is prepared.

2.2. Photovoltaic Properties

To investigate the potential application of GDTA as additive to improve the performance of OSCs, devices with a conventional configuration of ITO/PEDOT:PSS/PM6:Y6 (1:1.2 by weight ratio)/PDINO/Ag (**Figure 2**a,b) were fabricated and optimized by varying the processing additives and post thermal treatment following the method reported by Zou et al.[12] The typical current density–voltage (*J–V*) curves and the resulting photovoltaic parameters of the devices are summarized in Figure 2c and **Table 1**. The PM6:Y6-based devices delivered a

Table 1. Photovoltaic parameters of PM6:Y6 OSCs with and without GDTA..

Active layers	GDTA	V_{OC} [V]	J_{SC} [mA cm^{-2}]	FF [%]	PCE [%]	*Cal.* J_{SC} [b] [mA cm^{-2}]
PM6:Y6	0	0.83(0.829 ± 0.002)	25.5(25.3 ± 0.2)	74.5(74.3 ± 0.4)	15.8(15.6 ± 0.2)	25.0
(1:1.2)	2%	0.85(0.852 ± 0.002)	27.1(27.0 ± 0.2)	76.2(76.1 ± 0.4)	17.6(17.5 ± 0.1)[a]	26.6

[a] The average photovoltaic parameters were determined from the measurements of over 100 separate devices. [b] Calculated by integrating EQE curves.

PCE of 15.8% when 0.5% 1-chloronaphthalene (CN) (v/v) was employed as a solvent additive alongside annealing of the blend films at 110 °C for 10 min.[12] Based on the optimal device fabrication conditions, the photovoltaic performances of PM6:Y6-based OSCs were further studied by varying the content of GDTA (0.5–5% w/w relative to PM6). As shown in Figure 2c, Table 1, and Table S3 and Figure S4 (Supporting Information), the open-circuit voltages (V_{OC}s), J_{SC}s, and FFs of the OSCs were improved from 0.83 V, 25.5 mA cm^{-2} and 74.5% to 0.85 V, 27.1 mA cm^{-2} and 76.2% upon the addition of 2 wt% GDTA additives. This resulted in an increase in PCE from 15.8% to 17.6%. Further increase in GDTA content led to declined V_{OC} and FF values (0.84 V and 71.8% at 3% GDTA, 0.83 V and 70.0% at 5% GDTA).

To verify the reproducibility of the high performance, over 100 devices were fabricated under the optimal device fabrication condition with 2 wt% GDTA to get the statistical data (inset of Figure 2c). Finally, an average PCE of 17.5% was obtained and the best PCE was 17.6% with a V_{OC} of 0.85 V, a J_{SC} of 27.1 mA cm^{-2}, and an FF of 76.2%. The external quantum efficiencies (EQEs) of the OSCs were also measured to verify the accuracy of the *J*–*V* curves of PM6:Y6-based OSCs with and without GDTA. The PM6:Y6-based OSCs with 2% GDTA showed slightly enhanced EQEs in the range of 450–850 nm compared to that without GDTA (Figure 2d). The integrated current densities from the EQEs spectra were 25.0 and 26.6 mA cm^{-2} for the PM6:Y6-based devices without and with 2% GDTA, respectively, which agree well with those obtained from the *J*–*V* measurements. For comparison, the effect of GDZZ, which has the same backbone as GDTA but without radical side groups, on the photovoltaic performance of PM6:Y6-based OSCs was also investigated. The resulting devices with 2% GDZZ showed a slight decrease in their PCEs (from 15.8% to 15.1%) as compared to those without additives. (Figure S5 and Table S4, Supporting Information).

To investigate the effects of the addition of GDTA on the stability of the devices, the shelf life of the PM6:Y6-based devices with and without 2 wt% GDTA were monitored and compared. As presented in Figure S6 (Supporting Information), the PCEs of the OSCs with and without 2 wt% GDTA remained at about 88.9% and 87.4%, respectively, of their initial value after the devices were kept in a glovebox in the dark for 144 h. Meanwhile, the photostability of the OSCs fabricated from PM6:Y6 blends was also monitored under illumination with a 1 sun (100 mW cm^{-2}) white-light LED (LED color temperature: 6000 K, wavelength: 400–800 nm) at ambient temperature in a glovebox with oxygen and water contents less than 1 ppm. As shown in Figure S7 (Supporting Information), the PCEs of the OSCs with and without GDTA additives lost 16.1% and 21.7%, respectively, of their initial value after 68 h irradiation. This suggested that the OSCs fabricated from PM6:Y6 blends with GDTA presented enhanced photostability as compared with the devices without GDTA.

2.3. General Effectiveness of the GDTA Additives in Boosting the PCEs of the OSCs

To explore the applicability of GDTA to influence the performance of OSCs from different D:A materials systems, OSCs based on P3HT:PC_{71}BM, PTB7:PC_{61}BM, PTB7-Th:PC_{71}BM, PBDB-T:ITIC, J61:ITIC, PBDB-T:IT-4F, etc., were investigated. The devices were prepared by following the optimal device fabrication conditions for each D:A pair (Table S5, Supporting Information) and the added amount of GDTA was fixed at 2% (relative to the weight of donor polymers) to simplify the experiments (Table S6, Supporting Information). For comparison, the counterpart OSCs with Gxl and TEMPO as additives were also prepared and characterized. The parameters of the OSCs are summarized in Table S7 and Table S8 (Supporting Information), respectively. Interestingly, the performances of the OSCs derived from most of the D:A pairs were decreased upon the addition of Gxl or TEMPO (Tables S7 and S8, Supporting Information). As shown in **Figure 3** and Table S6 (Supporting Information), for the OSCs in which the major free charge recombination proceeds via the formation of T_1 (Figure 3, Class I).[40,52] their V_{OC}s increased along with the improvement of the J_{SC}s and FFs upon the addition of GDTA, resulting in substantial improvement in their PCEs by 7%–15%. Notably, the PCEs of the OSCs from PM6:BTP-eC9 blends were increased from 17.5% to 18.3% upon the addition of 0.5% GDTA. It is noticed that, with the addition of the GDTA additives, the enhancement of PCEs for PM6:BTP-eC9 is smaller than that of the PM6:Y6 system (0.8% vs 2%), which might be ascribed to their strongly suppressed (non-Langevin) recombination as compared with the PM6:Y6-based devices.[60] Therefore, there is only little room for the improvement in the PM6:BTP-eC9 system. On contrary, for the P3HT:PC_{71}BM- and PBDB-T:PC_{71}BM-based OSCs, in which T_1 formation was negligible (Figure 3, Class II),[52] the V_{OC} was decreased upon the addition of GDTA, while the J_{SC} and FF of the devices were slightly increased. The results indicated that the addition of GDTA should be effective for the OSCs derived from a broad range of D and A pairs, especially for the OSCs in which the major free charge recombination proceeds via the formation of T_1.

2.4. Influence of GDTA Addition on the Optical, Morphological, and Carrier Mobility Characteristics

In order to gain insight into the reasons for the improvement in the performances of OSCs when GDTA was used as a solid additive, we used the PM6:Y6 pair as a model system to thoroughly investigate the photophysics, nanomorphology, and charge dynamics of the blend films upon the addition of GDTA. First, we measured the absorption spectra of the blend films based on PM6:Y6

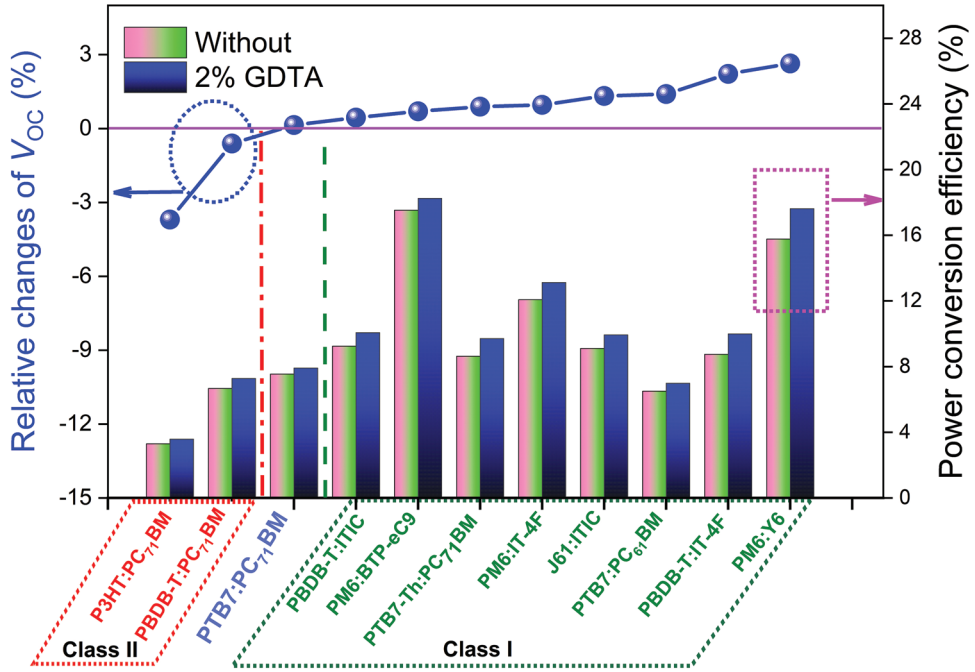

Figure 3. Relative changes of V_{OC} and PCEs of the OSCs from different D and A materials upon the addition of 2 wt% GDTA.

with and without GDTA. As shown in Figure S8 (Supporting Information), the PM6:Y6 blend films with 2% GDTA additives presented almost the same absorptance spectra as the original blend film. Next, we performed grazing-incidence wide-angle X-ray scattering (GIWAXS), atomic force microscopy (AFM) and transmission electron microscopy (TEM) measurements to compare the film morphology. The results indicate that the addition of 2 wt% GDTA into the PM6:Y6 blend films produced slightly pronounced reflections at 0.22 and 0.43 $Å^{-1}$, alongside the slight variation of the root-mean-square (RMS) roughness from 0.534 to 0.775 nm and similar morphology as well (Figure S9, Supporting Information). These indicated that the addition of GDTA had no marked influence on the nanomorphology and molecular packing of the blend films. Furthermore, the charge-transport measurements on the blend films with and without GDTA indicated that the addition of 2% GDTA into the PM6:Y6 blend films has no certifiable influence on charge-transport properties as very similar electron and hole mobilities are measured for devices with and without GDTA (Figure S10 and Tables S9 and S10, Supporting Information).[10] Overall, the above results indicated that the addition of GDTA does not alter the optical properties, blend morphology, and charge-carrier mobility of the PM6:Y6-based blend films, to an extent that justifies the main reasons for the enhancement of the V_{OC}, J_{SC}, and FFs of the OSCs (see detailed discussion in Note S2 in the Supporting Information).

2.5. Reduction of Nonradiative Energy Loss of the PM6:Y6 OSCs upon the Addition of GDTA

The Fourier-transform photocurrent spectroscopy external quantum efficiency (FTPS-EQE), electroluminescence (EL) spectra, and electroluminescence external quantum efficiency (EQE_{EL}) of the PM6:Y6-based OSCs, with and without GDTA, were further investigated and the results were presented in **Figure 4**. As shown in Figure 4a,b, both devices show almost the same FTPS-EQE and EL spectra. However, the OSCs from PM6:Y6 with 2% GDTA maintained a higher EQE_{EL} of 6.6×10^{-3}%, therefore, leading to the $V_{oc}^{non-rad}$ of 0.25 eV, calculated using the equation $V_{oc}^{non-rad} = -\frac{kT}{q}\ln(EQE_{EL})$,[31,61,62] which was lower by 0.02 eV than that of the PM6:Y6-based devices without GDTA (Figure 4c). The result agreed well with the 20 mV improvement in V_{OC} (Table 1), indicating that the $E_{loss}^{non-rad}$ of the PM6:Y6- based OSCs was reduced upon adding GDTA. Likewise, the power-law J_{SC} dependence on the irradiating light intensity (P_{light}) ($J_{SC} \propto P_{light}^{\alpha}$) of the OSCs of PM6:Y6 films with and without 2% GDTA additives, were also investigated. The α value obtained for the OSCs with 2% GDTA additives (0.970) was higher than that of the OSCs without GDTA (0.926) (Figure S11, Supporting Information), suggesting that the GDTA addition could result in substantial suppression of the nongerminate recombination of free charge carriers.[63,64]

To get more insight into the $E_{loss}^{non-rad}$ of the PM6:Y6 OSCs upon the addition of GDTA, femtosecond/nanosecond transient absorption (fs-TA/ns-TA) spectroscopic measurements were further performed, and the results were presented in Figure S12 (Supporting Information). As shown in Figure S12a (Supporting Information), in the initial stages, an excited-state absorption band (ESA) at 1550 nm, was monitored from 0.5 to 10 ps. As time progressed from 10 to 1510 ps, an ESA feature at around 1450 nm was observed, and then the ESA intensity increased afterward. According to Zhang et al., the ESA feature at 1550 nm can be assigned to the intramoiety excited (i-EX) state.[65] The ESA feature at round 1450 nm can be assigned to T_1 on Y6 via the triplet sensitization measurements of neat Y6 with platinum octaethylporphyrin (PtOEP) (Figure S12b, Supporting

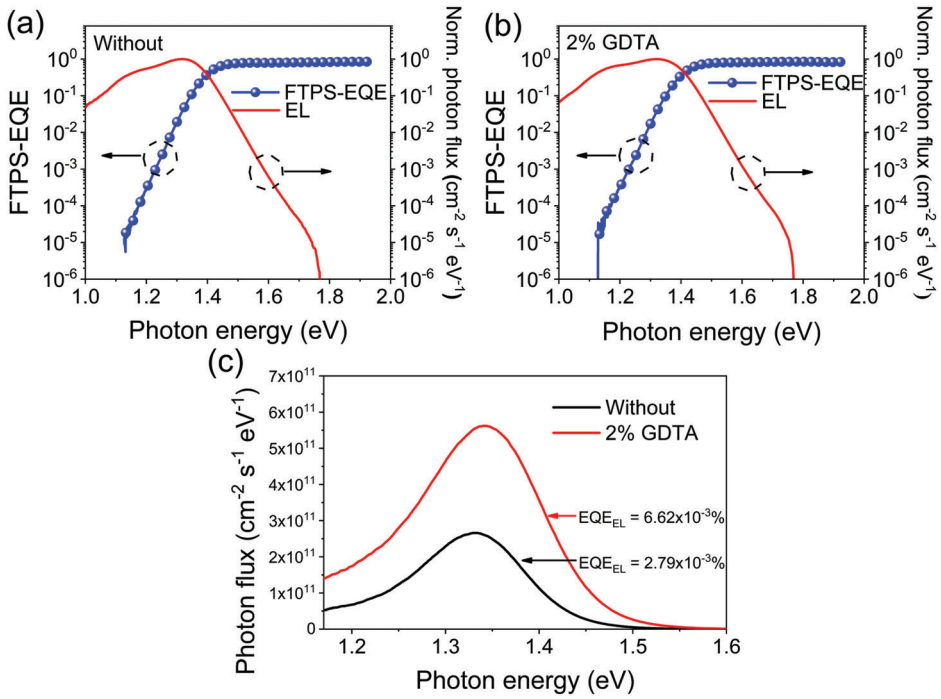

Figure 4. a) EL and FTPS-EQE of the PM6:Y6-based OSCs without GDTA. b) EL and FTPS-EQE of the PM6:Y6-based OSCs with 2% GDTA. c) EQE_{EL} of the PM6:Y6-based OSCs without and with 2% GDTA under the current density of 50 mA cm^{-2}.

Information), which was similar to the data reported in the literature.[40] Figure S12c,d (Supporting Information) shows the ns-TA behaviors of the PM6:Y6 blends, with and without GDTA, under a picosecond pulse excitation of weak fluence at 670 nm (≈100 ps, ≈ 2 μJ cm^{-2}, LDH, Pico quant). The spectra in the long-wavelength range (1100–1600 nm) were magnified by a factor of 10 for clarity. Upon the addition of GDTA, the amplitude of the triplet signals centered at ≈1450 nm decreased while the ESA signal at 770 nm increased. ESA at 770 nm on the time scale of ns or later was contributed by the free polarons postcharge separation.[65] The increase of the EAS at 770 nm indicates that the addition of GDTA likely promoted charge generation. In parallel, the time-resolved traces probed at 1450 nm from the two samples suggest that the decay of the triplet became faster with the addition of GDTA, suggesting that the addition of GDTA likely decreased the population and shortened the lifetime of the T_1 on Y6 (Figures S12e,f, Supporting Information). While the triplet-charge annihilation (TCA) occurs via a charge and one triplet exciton as suggested by Gillett et al.[40] and Neher et al.[43] and the additional channel of spin conversion was not introduced to change the TCA reaction rate constant, it would be an inevitable deduction that the promoted charge generation contributes to the increase of the free charge population, thus resulting in the shortening of the lifetime of the T_1 on Y6 (see detailed discussion in Note S3 in the Supporting Information). The results indicate that the nonradiative recombination of free charge carriers in the representative OSCs from PM6:Y6 blends might be predominantly through back electron transfer from triplet CT states to low-lying triplet excitons of Y6 as suggested by Gillett et al.[40] It also suggests that the addition of the GDTA additives might result in the suppression of ^{3}CT's decay to T_1 on Y6.

3. Discussion

The possible reasons behind the effect of GDTA on the performance of OSCs are discussed as follows. First, it may be speculated that the enhancement of the PCEs of the OSCs upon the addition of GDTA is related to electrical doping or improvements in charge-carrier mobilities. We argue that none of these mechanisms can be responsible for the simultaneous improvement of the J_{SC} and V_{OC}.[34,66,67] We also measured electron and hole mobilities (Tables S9 and S10, Supporting Information) and found the values to be unaffected by the introduction of GDTA. Likewise, the energy levels of GDTA relative to PM6:Y6 as shown in Figure 1d do not meet requirements for n-type ($HOMO_{dopant}$ > $LUMO_{host}$) or p-type ($LUMO_{dopant}$ < $HOMO_{host}$) doping, therefore it cannot be considered as a molecular dopant. In any case, and if it could act as a molecular dopant, its effect would not be necessarily positive and impactful on the V_{OC}. This is because previous works on PM6:Y6 have shown that electrical doping may have both positive and negative effects on the performance (depending on the device architecture), and the V_{OC} is not affected by the doping (Figures S13–S15 and Table S11; see detailed discussion in Note S4 in the Supporting Information).[66–68]

Another potentially responsible process for the improvement upon the addition of GDTA may be the mechanism of the spin radical facilitating intersystem crossing conversion of ^{3}CT to ^{1}CT proposed by Vardeny et al.[54] In that case, however, it is not entirely clear as to why and how the radical additives asymmetrically regulate the forward and reverse intersystem crossing rates between the ^{1}CT and ^{3}CT.[54] In the OSCs fabricated from PM6:Y6, our data shows that the $E_{loss}^{non-rad}$ and T_1 on Y6 were reduced upon addition of GDTA (Figure 4c; Figure S12e, Supporting

Information). From these finding one may speculate that the spin-½ radical of GDTA may facilitate the conversion of the ^{3}CT to ^{1}CT and decreases the density of ^{3}CT, thus reducing the T_1 population on Y6 by slowing down the BCT from ^{3}CT to T_1. Therefore, the $E_{loss}^{non-rad}$ via TCA is decreased and hence an improvement in the V_{OC}s. Our further investigation suggests that this argument may not be true. By following the line of said argument, the addition of TEMPO is expected to result in the increase of the PCEs of the PM6:Y6-based OSCs. However, it is noted that the introduction of a similar amount of the small molecular radical TEMPO, which presents almost the same SOMO energy level as the dangling TEMPO in the GDTA, results in a slight decrease, rather than an increase of the PCEs of PM6:Y6 devices (Figure S15 and Tables S8 and S11, Supporting Information). Additionally, it is also inconvincible that GDTA only facilitates the intersystem crossing conversion of ^{3}CT to ^{1}CT for the OSCs from Class I, but not for Class II, photovoltaic D:A systems.

Based on the above discussion, we conclude that the improvement in the devices with GDTA is most likely not related to the enhanced intersystem crossing conversion of ^{3}CT to ^{1}CT. Instead, one plausible explanation for the improvement with GDTA is the enhancement of charge generation yield, which also reduces bimolecular recombination. As discussed in the citations,[36,42,70] the charge generation quantum yield depends on the ratio of the dissociation rate of the CT states to the overall decay rate of the CT states. Enhancement of the CT dissociation rate (which results in improved charge generation) indeed improves the J_{SC} and FF, however, the V_{OC} remains only dependent on the nonradiative decay rate of the CT states. In accordance with our EQE_{EL} results and the V_{OC}, J_{SC} and FF improvement as well, we suggest that GDTA slows down the CT state's decay. This can be suppression of vibrationally induced nonradiative decay of ^{1}CT or a reduction in the back transfer of ^{3}CT to the T_1 excitons loss channel upon the addition of the GDTA additives. Meanwhile, the slight improvement in V_{OC} (increasing the EQE_{EL} by a factor of ≈2.5) and partially slowing down the formation of T_1 on Y6, might be ascribed to the most likely formation of the GDTA aggregates, which inevitably have some shared interface with the donor and acceptor (Figure S16 and see detailed discussion in Note S5 in the Supporting Information). Further details of these processes remain unclear with some open questions for future studies.

4. Conclusion

A nitroxide radical conjugated polymer, GDTA, bearing TEMPO in the side chains, was successfully developed and characterized. Upon the addition of 2 wt% GDTA (with weight ratio relative to PM6), the PCEs of PM6:Y6-based OSCs were improved from 15.8% to 17.6% alongside the enhancement of the photostability, without certifiable changes in optical, morphological, and charge-transport characteristics. The improvement of the FFs and J_{SC}s as well as a small enhancement in V_{OC}s of the representative OSCs from PM6:Y6, ascribed to the reduced nonradiative CT decay, were observed and supported by a range of optical and electrical spectroscopic measurements. Besides, the general effectiveness of the GDTA additive to improve the photovoltaic performances of the OSCs based on various D:A pairs, in which the major free charge recombination proceeds via the formation of T_1 excitons, has been verified. Especially, the OSCs based on the PM6: BTP-eC9 blends with 0.5% GDTA could deliver a maximum PCE of 18.3%. To the best of our knowledge, this is the first report on a radical conjugated polymer used as an additive to extensively and effectively boost PCEs of OSCs based on a broad range of D:A materials through the suppression of T_1 formation. This study not only opens a new avenue for further improvement of the photovoltaic performances of OSCs, but also provides an important design insight for such kind of radical polymer additives to efficiently suppress the energy loss via T_1 in OSCs.

Supporting Information

Supporting Information is available from the Wiley Online Library or from the author.

Acknowledgements

F.S., P.G., and X.Q. contributed equally to this work. This work was supported by the Industrial Guidance Project for Colleges and Universities of Gansu Province (2020C-07), the National Nature Science Foundation of China (62164007 and 51903112), and Tianyou Youth Talent Lift Program of Lanzhou Jiaotong University. H.Y.W. acknowledges the financial support from the National Research Foundation (NRF) of Korea (2019R1A2C2085290 and 2019R1A6A1A11044070). E.W. acknowledges the financial support from the K&A Wallenberg Foundation (2017.0186 and 2016.0059), the Swedish Energy Agency (P2021-90067), the Swedish Research Council (2016-06146 and 2019-04683), and Formas. X.F.Q. acknowledges the Open Project Program of Wuhan National Laboratory for Optoelectronics (No. 2019WNLOKF016). A.A. is a Sêr Cymru II Rising Star Fellow and acknowledges EPSRC Program Grant EP/T028511/1 Application Targeted Integrated Photovoltaics. Y.X. gratefully acknowledges the support from the Instrument Analysis Center of Lanzhou Jiaotong University.

Conflict of Interest

The authors declare no conflict of interest.

Data Availability Statement

The data that support the findings of this study are available from the corresponding author upon reasonable request.

Keywords

low-lying triplets, nitroxide radical conjugated polymers, nonradiative energy loss, organic solar cells, solid additives

Received: December 24, 2022
Revised: February 23, 2023
Published online:

[1] G. Yu, J. Gao, J. C. Hummelen, F. Wudl, A. J. Heeger, *Science* **1995**, *270*, 1789.
[2] P. Cheng, G. Li, X. Zhan, Y. Yang, *Nat. Photonics* **2018**, *12*, 131.
[3] A. Armin, W. Li, O. J. Sandberg, Z. L. Ding, J. Nelson, D. Neher, K. Vandewal, S. Shoaee, T. Wang, H. Ade, T. Heumüller, C. Brabec, P. Meredith, *Adv. Energy Mater.* **2021**, *11*, 20003570.

[4] G. Burwell, N. Burridge, E. Bond, W. Li, P. Meredith, A. Armin, *Adv. Electron. Mater.* **2021**, *7*, 2100192.
[5] J. C. Hummelen, B. W. Knight, F. LePeq, F. Wudl, J. Yao, C. L. Wilkins, *J. Org. Chem.* **1995**, *60*, 532.
[6] D. Qian, W. Ma, Z. Li, X. Guo, S. Zhang, L. Ye, H. Ade, Z. Tan, J. Hou, *J. Am. Chem. Soc.* **2013**, *135*, 8464.
[7] L. Huo, T. Liu, X. Sun, Y. Cai, A. J. Heeger, Y. Sun, *Adv. Mater.* **2015**, *27*, 2938.
[8] Y. Lin, J. Wang, Z.-G. Zhang, H. Bai, Y. Li, D. Zhu, X. Zhan, *Adv. Mater.* **2015**, *27*, 1170.
[9] H. Bin, Z.-G. Zhang, L. Gao, S. Chen, L. Zhong, L. Xue, C. Yang, Y. Li, *J. Am. Chem. Soc.* **2016**, *138*, 4657.
[10] W. Zhao, S. Li, H. Yao, S. Zhang, Y. Zhang, B. Yang, J. Hou, *J. Am. Chem. Soc.* **2017**, *139*, 7148.
[11] Z. Luo, R. Ma, T. Liu, J. Yu, Y. Xiao, R. Sun, G. Xie, J. Yuan, Y. Chen, K. Chen, G. Chai, H. Sun, J. Min, J. Zhang, Y. Zou, C. Yang, X. Lu, F. Gao, H. Yan, *Joule* **2020**, *4*, 1236.
[12] J. Yuan, Y. Zhang, L. Zhou, G. Zhang, H.-L. Yip, T.-K. Lau, X. Lu, C. Zhu, H. Peng, P. A. Johnson, M. Leclerc, Y. Cao, J. Ulanski, Y. Li, Y. Zou, *Joule* **2019**, *3*, 1140.
[13] G. Li, V. Shrotriya, J. Huang, Y. Yao, T. Moriarty, K. Emery, Y. Yang, *Nat. Mater.* **2005**, *4*, 864.
[14] J. K. Lee, W. L. Ma, C. J. Brabec, J. Yuen, J. S. Moon, J. Y. Kim, K. Lee, G. C. Bazan, A. J. Heeger, *J. Am. Chem. Soc.* **2008**, *130*, 3619.
[15] T. Kietzke, D. Neher, K. Landfester, R. Montenegro, R. Güntner, U. Scherf, *Nat. Mater.* **2003**, *2*, 408.
[16] Z. He, C. Zhong, S. Su, M. Xu, H. Wu, Y. Cao, *Nat. Photonics* **2012**, *6*, 591.
[17] K. Yoshikawa, H. Kawasaki, W. Yoshida, T. Irie, K. Konishi, K. Nakano, T. Uto, D. Adachi, M. Kanematsu, H. Uzu, K. Yamamoto, *Nat. Energy* **2017**, *2*, 17032.
[18] J. Jeong, M. Kim, J. Seo, H. Lu, P. Ahlawat, A. Mishra, Y. Yang, M. A. Hope, F. T. Eickemeyer, M. Kim, Y. J. Yoon, I. W. Choi, B. P. Darwich, S. J. Choi, Y. Jo, J. H. Lee, B. Walker, S. M. Zakeeruddin, L. Emsley, U. Rothlisberger, A. Hagfeldt, D. S. Kim, M. Grätzel, J. Y. Kim, *Nature* **2021**, *592*, 381.
[19] NREL, Best Research-Cell Efficiencies, https://www.nrel.gov/pv/assets/pdfs/cell-pv-eff-emergingpv.pdf (accessed: March 2023).
[20] M. Hilczer, M. Tachiya, *J. Phys. Chem. C* **2010**, *114*, 6808.
[21] S. D. Dimitrov, J. R. Durrant, *Chem. Mater.* **2014**, *26*, 616.
[22] P. C. Y. Chow, S. Gélinas, A. Rao, R. H. Friend, *J. Am. Chem. Soc.* **2014**, *136*, 3424.
[23] J. Yao, T. Kirchartz, M. S. Vezie, M. A. Faist, W. Gong, Z. He, H. Wu, J. Troughton, T. Watson, D. Bryant, J. Nelson, *Phys. Rev. Appl.* **2015**, *4*, 014020.
[24] D. Qian, Z. Zheng, H. Yao, W. Tress, T. R. Hopper, S. Chen, S. Li, J. Liu, S. Chen, J. Zhang, X.-K. Liu, B. Gao, L. Ouyang, Y. Jin, G. Pozina, I. A. Buyanova, W. M. Chen, O. Inganäs, V. Coropceanu, J.-L. Bredas, H. Yan, J. Hou, F. Zhang, A. A. Bakulin, F. Gao, *Nat. Mater.* **2018**, *17*, 703.
[25] A. Rao, P. C. Y. Chow, S. Gélinas, C. W. Schlenker, C.-Z. Li, H.-L. Yip, A. K.-Y. Jen, D. S. Ginger, R. H. Friend, *Nature* **2013**, *500*, 435.
[26] W. Chang, D. N. Congreve, E. Hontz, M. E. Bahlke, D. P. McMahon, S. Reineke, T. C. Wu, V. Bulovic, T. V. Voorhis, M. A. Baldo, *Nat. Commun.* **2015**, *6*, 6415.
[27] K. N. Schwarz, P. B. Geraghty, D. J. Jones, T. A. Smith, K. P. Ghiggino, *J. Phys. Chem. C* **2016**, *120*, 24002.
[28] Y. Li, L. Zhong, B. Gautam, H.-J. Bin, J.-D. Lin, F.-P. Wu, Z. Zhang, Z.-Q. Jiang, Z.-G. Zhang, K. Gundogdu, Y. Li, L.-S. Liao, *Energy Environ. Sci.* **2017**, *10*, 1610.
[29] Y. Xie, W. Wang, W. Huang, F. Lin, T. Li, S. Liu, X. Zhan, Y. Liang, C. Gao, H. Wu, Y. Cao, *Energy Environ. Sci.* **2019**, *12*, 3556.
[30] C. Liu, K. Huang, W.-T. Park, M. Li, T. Yang, X. Liu, L. Liang, T. Minari, Y.-Y. Noh, *Mater. Horiz.* **2017**, *4*, 608.
[31] S. Liu, J. Yuan, W. Deng, M. Luo, Y. Xie, Q. Liang, Y. Zou, Z. He, H. Wu, Y. Cao, *Nat. Photonics* **2020**, *14*, 300.
[32] Q. Liu, Y. Jiang, K. Jin, J. Qin, J. Xu, W. Li, J. Xiong, J. Liu, Z. Xiao, K. Sun, S. Yang, X. Zhang, L. Ding, *Sci. Bull.* **2020**, *65*, 272.
[33] Y. Cui, H. Yao, J. Zhang, K. Xian, T. Zhang, L. Hong, Y. Wang, Y. Xu, K. Ma, C. An, C. He, Z. Wei, F. Gao, J. Hou, *Adv. Mater.* **2020**, *32*, 1908205.
[34] Y. Lin, M. I. Nugraha, Y. Firdaus, A. D. Scaccabarozzi, F. Aniés, A.-H. Emwas, E. Yengel, X. Zheng, J. Liu, W. Wahyudi, E. Yarali, H. Faber, O. M. Bakr, L. Tsetseris, M. Heeney, T. D. Anthopoulos, *ACS Energy Lett.* **2020**, *5*, 3663.
[35] P. Bi, S. Zhang, Z. Chen, Y. Xu, Y. Cui, T. Zhang, J. Ren, J. Qin, L. Hong, X. Hao, J. Hou, *Joule* **2021**, *5*, 2408.
[36] A. Armin, N. Zarrabi, O. J. Sandberg, C. Kaiser, S. Zeiske, W. Li, P. Meredith, *Adv. Energy Mater.* **2020**, *10*, 2001828.
[37] J. C. Blakesley, D. Neher, *Phys. Rev. B* **2011**, *84*, 075210.
[38] F. D. Eisner, M. Azzouzi, Z. Fei, X. Hou, T. D. Anthopoulos, T. J. S. Dennis, M. Heeney, J. Nelson, *J. Am. Chem. Soc.* **2019**, *141*, 6362.
[39] X. K. Chen, V. Coropceanu, J. L. Brédas, *Nat. Commun.* **2018**, *9*, 5295.
[40] A. J. Gillett, A. Privitera, R. Dilmurat, A. Karki, D. Qian, A. Pershin, G. Londi, W. K. Myers, J. Lee, J. Yuan, S.-J. Ko, M. K. Riede, F. Gao, G. C. Bazan, A. Rao, T.-Q. Nguyen, D. Beljonne, R. H. Friend, *Nature* **2021**, *597*, 666.
[41] Q. Liu, S. Smeets, S. Mertens, Y. Xia, A. Valencia, J. D'Haen, W. Maes, K. Vandewal, *Joule* **2021**, *5*, 2365.
[42] A. Armin, J. R. Durrant, S. Shoaee, *J. Phys. Chem. C* **2017**, *121*, 13969.
[43] L. Perdigón-Toro, L. Q. Phuong, S. Zeiske, K. Vandewal, A. Armin, S. Shoaee, D. Neher, *ACS Energy Lett.* **2021**, *6*, 557.
[44] N. An, Y. Cai, H. Wu, A. Tang, K. Zhang, X. Hao, Z. Ma, Q. Guo, H. S. Ryu, H. Y. Woo, Y. Sun, E. Zhou, *Adv. Mater.* **2020**, *32*, 2002122.
[45] J. Zhou, P. Lei, Y. Geng, Z. He, X. Li, Q. Zeng, A. Tang, E. Zhou, *J. Mater. Chem. A* **2022**, *10*, 9869.
[46] D. D. Nuzzo, A. Aguirre, M. Shahid, V. S. Gevaerts, S. C. J. Meskers, R. A. J. Janssen, *Adv. Mater.* **2010**, *22*, 4321.
[47] L. Xue, Y. Yang, J. Xu, C. Zhang, H. Bin, Z.-G. Zhang, B. Qiu, X. Li, C. Sun, L. Gao, J. Yao, X. Chen, Y. Yang, M. Xiao, Y. Li, *Adv. Mater.* **2017**, *29*, 1703344.
[48] C. Sun, F. Pan, S. Chen, R. Wang, R. Sun, Z. Shang, B. Qiu, J. Min, M. Lv, L. Meng, C. Zhang, M. Xiao, C. Yang, Y. Li, *Adv. Mater.* **2019**, *31*, 1905480.
[49] R. Wang, J. Xu, L. Fu, C. Zhang, Q. Li, J. Yao, X. Li, C. Sun, Z.-G. Zhang, X. Wang, Y. Li, J. Ma, M. Xiao, *J. Am. Chem. Soc.* **2021**, *143*, 4359.
[50] Z. Chen, X. Chen, Z. Jia, G. Zhou, J. Xu, Y. Wu, X. Xia, X. Li, X. Zhang, C. Deng, Y. Zhang, X. Lu, W. Liu, C. Zhang, Y. Yang, H. Zhu, *Joule* **2021**, *5*, 1832.
[51] Y. Zhang, T. P. Basel, B. R. Gautam, X. Yang, D. J. Mascaro, F. Liu, Z. V. Vardeny, *Nat. Commun.* **2012**, *3*, 1043.
[52] Y. Zhang, G. Hukic-Markosian, D. Mascaro, Z. V. Vardeny, *Synth. Met.* **2010**, *160*, 262.
[53] J. M. Cho, D. S. Kim, S. Bae, S.-J. Moon, W. S. Shin, D. H. Kim, S. H. Kim, A. Sperlich, S. Väth, V. Dyakonov, J.-K. Lee, *Org. Electron.* **2015**, *27*, 119.
[54] T. Basel, U. Huynh, T. Zheng, T. Xu, L. Yu, Z. V. Vardeny, *Adv. Funct. Mater.* **2015**, *25*, 1895.
[55] P. Gao, J. Tong, P. Guo, J. Li, N. Wang, C. Li, X. Ma, P. Zhang, C. Wang, Y. Xia, *J. Polym. Sci., Part A* **2018**, *56*, 85.
[56] B. Neises, W. Steglich, *Angew. Chem., Int. Ed. Engl.* **1978**, *17*, 522.
[57] G. R. Luckhurst, *Mol. Phys.* **1965**, *9*, 179.
[58] X. Pang, W. J. Jin, *New J. Chem.* **2015**, *39*, 5477.
[59] J. Pommerehne, H. Vestweber, W. Guss, R. F. Mahrt, H. Bässler, M. Porsch, J. Daub, *Adv. Mater.* **1995**, *7*, 551.
[60] W. Li, S. Zeiske, O. J. Sandberg, D. B. Riley, P. Meredith, A. Armin, *Energy Environ. Sci.* **2021**, *14*, 6484.

[61] Q. Liu, Y. Wang, J. Fang, H. Liu, L. Zhu, X. Guo, M. Gao, Z. Tang, L. Ye, F. Liu, M. Zhang, Y. Li, *Nano Energy* **2021**, *85*, 105963.
[62] A. Karki, J. Vollbrecht, A. L. Dixon, N. Schopp, M. Schrock, G. N. M. Reddy, T.-Q. Nguyen, *Adv. Mater.* **2019**, *31*, 1903868.
[63] Y. Li, H. Meng, T. Liu, Y. Xiao, Z. Tang, B. Pang, Y. Li, Y. Xiang, G. Zhang, X. Lu, G. Yu, H. Yan, C. Zhan, J. Huang, J. Yao, *Adv. Mater.* **2019**, *31*, 1904585.
[64] K. Li, Y. Wu, Y. Tang, M.-A. Pan, W. Ma, H. Fu, C. Zhan, J. Yao, *Adv. Energy Mater.* **2019**, *9*, 1901728.
[65] R. Wang, C. Zhang, Q. Li, Z. Zhang, X. Wang, M. Xiao, *J. Am. Chem. Soc.* **2020**, *142*, 12751.
[66] G. Zuo, Z. Li, O. Andersson, H. Abdalla, E. Wang, M. Kemerink, *J. Phys. Chem. C* **2017**, *121*, 7767.
[67] Y. Zhang, H. Zhou, J. Seifter, L. Ying, A. Mikhailovsky, A. J. Heeger, G. C. Bazan, T. Nguyen, *Adv. Mater.* **2013**, *25*, 7038.
[68] Y. Lin, Y. Firdaus, M. I. Nugraha, F. Liu, S. Karuthedath, A.-H. Emwas, W. Zhang, A. Seitkhan, M. Neophytou, H. Faber, E. Yengel, I. McCulloch, L. Tsetseris, F. Laquai, T. D. Anthopoulos, *Adv. Sci.* **2020**, *7*, 1903419.
[69] M. Nyman, O. J. Sandberg, W. Li, S. Zeiske, R. Kerremans, P. Meredith, A. Armin, *Sol. RRL* **2021**, *5*, 2100018.
[70] A. Armin, W. Li, O. J. Sandberg, Z. Xiao, L. Ding, J. Nelson, D. Neher, K. Vandewal, S. Shoaee, T. Wang, H. Ade, T. Heumüller, C. Brabec, P. Meredith, *Adv. Energy Mater.* **2021**, *11*, 20003570.